

Potential risk resulting from the influence of static magnetic field upon living organisms. Numerically simulated effects of the static magnetic field upon simple alkanols

Wojciech Ciesielski¹, Tomasz Girek¹, Zdzisław Oszczęda²,
Jacek A. Soroka³, Piotr Tomasiak²

1 Institute of Chemistry, Jan Długosz University, 42–201 Częstochowa, Poland **2** Nantes Nanotechnological Systems, 59–700 Bolesławiec, Poland **3** Scientific Society of Szczecin, 71–481 Szczecin, Poland

Corresponding author: Wojciech Ciesielski (w.ciesielski@interia.pl)

Academic editor: Josef Settele | Received 24 October 2021 | Accepted 3 April 2022 | Published 13 June 2022

Citation: Ciesielski W, Girek T, Oszczęda Z, Soroka JA, Tomasiak P (2022) Potential risk resulting from the influence of static magnetic field upon living organisms. Numerically simulated effects of the static magnetic field upon simple alkanols. *BioRisk* 18: 35–55. <https://doi.org/10.3897/biorisk.18.76997>

Abstract

Background: Recognising effects of static magnetic field (SMF) of varying flux density on flora and fauna is attempted. For this purpose, the influence of static magnetic field upon molecules of lower alkanols i.e. methanol, ethanol, propan-1-ol, propan-2-ol, butan-1-ol, *S*-butan-2-ol, isobutanol and *tert*-butanol is studied.

Methods: Computations of the effect of real SMF 0.0, 0.1, 1, 10 and 100 AFU (Arbitrary Field Unit; here 1AFU > 1000 T) flux density were performed *in silico* (computer vacuum), involving advanced computational methods.

Results: SMF polarises molecules depending on applied flux density, but it neither ionises nor breaks valence bonds. Some irregularities in the changes of positive and negative charge densities and bond lengths provide evidence that molecules slightly change their initially fixed positions with respect to the force lines of the magnetic field. Length of some bonds and bond angles change with an increase in the applied flux density, providing, in some cases, polar interactions between atoms through space.

Conclusions: Since SMF produced and increase in the negative charge density at the oxygen atom of the hydroxyl group and elongated the –O–H bond length, these results show that SMF facilitates metabolism of the alkanols.

Keywords

Butanols, ethanol, methanol, organisms, propanols, static magnetic field

Introduction

Modern technologies and technical solutions in several areas of our everyday life result in considerable environmental pollution with magnetic fields (Hamza et al. 2002; Rankovic and Radulovic 2009; Committee to Assess the Current Status and Future Direction of High Magnetic Field Science in the United States 2013; Bao and Guo 2021; Tang et al. 2021). Recent studies showed an eminent effect of the static magnetic field (SMF) upon various micro-organisms, also on the colonising organisms of flora and fauna (Jaworska et al. 2014; Jaworska et al. 2016; Jaworska et al. 2017; Beretta et al. 2019). Numerous studies of the origin and mechanisms of observed effects pointed to a generation of free radicals which could interact with biological systems (Steiner and Ulrich 1989; Kohno et al. 2000; Woodward 2002; Buchachenko 2009; Buchachenko et al. 2012; Buchachenko 2014). The role of metal ions was also taken under consideration (Andreini et al. 2008; Rittie and Perbal 2008; Buchachenko 2016; Letuta and Berdinskiy 2017). It was found that SMF polarised molecules depending on the applied flux density, but causes neither ionisation nor breaking valence bonds of those molecules (Ciesielski et al. 2021).

Our former preliminary studies on the effect of SMF-treated water upon entomopathogenic organisms (Jaworska et al. 2017) and on functional properties of selected cosmetics (Zamiatała et al. 2013) suggest a necessity of an insight into the role of SMF in a modification of the molecular structure of simple molecules and interaction taking place in their combinations. For that purpose, numerical simulations of the real effect SMF of 0.0, 0.1, 1, 10 and 100 T were performed in a computer vacuum for single and grouped-in-three molecules of oxygen, nitrogen, water, carbon dioxide, ammonia and methane. Additionally, in this paper, T (Tesla) values were employed as commonly accepted units of the SMF flux density. However, since the response of the applied computational programme to the magnitudes of applied flux density remained unknown, the flux densities were expressed in terms of Arbitrary Field Units (AFU).

Organisms belonging to flora and fauna contain, amongst others, compounds bearing the hydroxyl groups bound to the sp^3 carbon atoms. They are alcohols. These in the flora organisms spread into sugar alcohols (Lewis and Smith 1967), fatty alcohols (Rowland and Domerque 2012) and steroid alcohols (Dinan et al. 2001). Similar types of alcohols reside in the fauna including human organisms.

Under normal conditions in the human organism, up to 0.15 ppm of so-called physiological ethanol is formed mainly through fatty acid synthesis, glycerolipid metabolism and bile acid biosynthesis pathways (Woronowicz 2003; Wade 2021).

In this paper, the effect of SMF of flux density from 0 to 100 AFU is recognised upon simple primary, secondary and tertiary C_1 to C_4 alkanols as the model compounds for the alcohols of more complex structure residing in the flora and fauna organisms. For this purpose, advanced numerical simulations of the effect were employed.

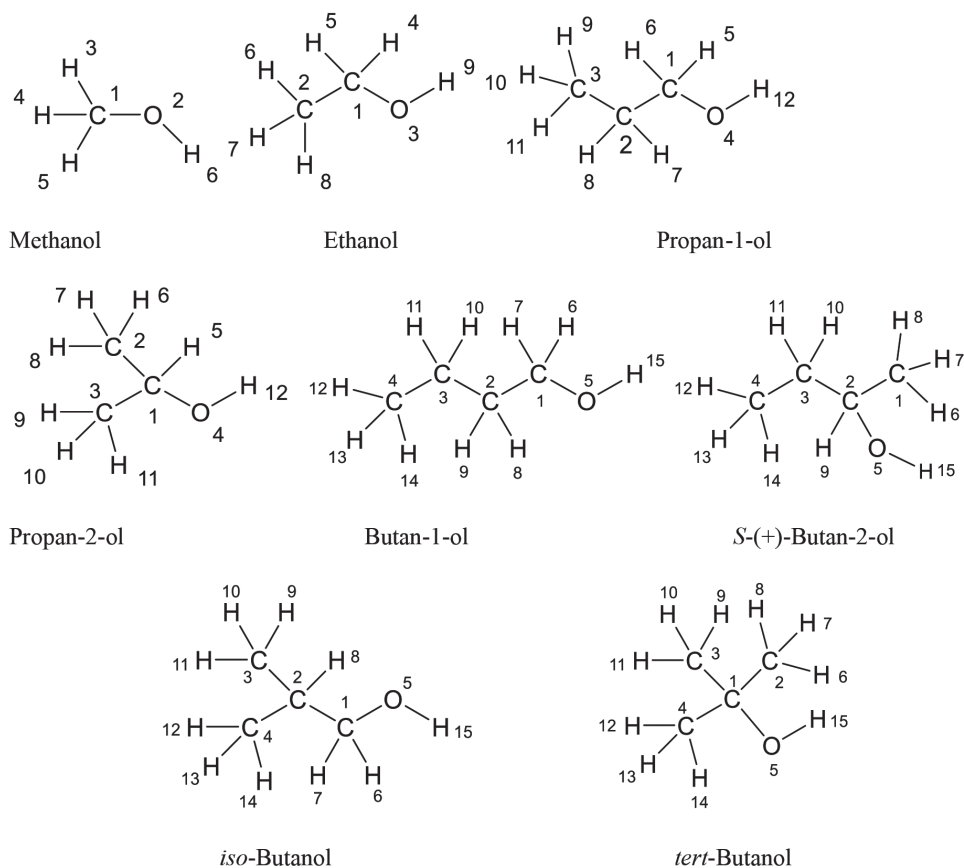


Figure 1. Alkanols under consideration and applied numbering of atoms in particular molecules.

Numerical computations

Molecular structures were drawn using the Fujitsu SCIGRESS 2.0 software (Froimowitz 1993; Marchand et al. 2014.). Their principal symmetry axes were orientated along the x-axis of the Cartesian system. Molecules of alcohols were situated inside of a three-axial ellipsoid. The longest axis of that ellipsoid was accepted as the x-axis and the shortest quasi-perpendicular axis considered as the z-axis. The magnetic field was fixed in the same direction, along the x-axis with the south pole from the left side. Thus, the methanol molecule was so orientated along its C-O bond and the remaining alcohols along their longest carbon chain. The magnetic field was fixed in the same direction with the south pole from the left side. Subsequently, involving Gaussian 0.9 software equipped with the 6-31G** basis (Frisch et al. 2016), the molecules were optimised and all values of bond length, dipole moment, heat of formation, bond energy and total energy for systems were computed.

In the consecutive steps, the influences of the static magnetic field (SMF) upon optimised molecules were computed with Amsterdam Modelling Suite software (Farberovich

and Mazalova 2016; Charistos and Muñoz-Castro 2019) and the NR_LDOTB (non-relativistically orbital momentum L-dot-B) method (Glendening et al. 1987; Carpenter and Weinhold 1988). Following that step, values of bond length, dipole moment, heat of formation equal to the energy of dissociation and charges at the atoms were calculated using Gaussian 0.9 software equipped with the 6-31G** basis (Marchand et al. 2014).

Results

Numerical simulations were performed for alkanols presented in Fig. 1.

Table 1 presents values of heat of formation and dipole moments for those alkanols placed in the SMF of flux density ranging from 0 (control sample) to 100 AFU.

Subsequent Tables contain computed values of charge density at particular atoms and bond lengths between atoms in methanol (Tables 2, 3), in ethanol (Tables 4, 5), in propan-1-ol (Tables 6, 7).

Table 1. Effect of SMF of increasing flux density upon heat of formation and dipole moment of alcohols.

Alcohol	Heat of formation [kJ·mol ⁻¹] at SMF flux density [AFU]					Dipole moment [D] at SMF flux density [AFU]				
	0	0.1	1.0	10	100*	0	0.1	1.0	10	100*
Methanol	-201.8	-195.3	-158.2	-114.2	-103.5 (49%)	1.94	2.03	2.15	2.36	3.01 (55%)
Ethanol	-238.8	-230.5	-219.8	-203.5	-151.1 (37%)	1.81	1.83	1.90	2.11	2.68 (42%)
Propan-1-ol	-251.7	-248.6	-231.2	-205.6	-171.6 (32%)	1.87	1.89	1.99	2.18	2.38 (27%)
Propan-2-ol	-271.5	-270.6	-263.8	-249.2	-199.3 (27%)	1.92	1.95	1.99	2.08	2.22 (16%)
Butan-1-ol	-276.1	-271.1	-253.6	-214.3	-161.1 (42%)	1.79	1.83	1.99	2.07	2.25 (26%)
S-Butan-2-ol	-302.8	-298.5	-278.2	-264.5	-211.6 (30%)	2.10	2.13	2.26	2.48	2.79 (33%)
iso-butanol	-285.1	-283.3	-279.2	-263.4	-183.3 (36%)	1.98	2.03	2.09	2.18	2.32 (17%)
tert-Butanol	-312.7	-310.2	-281.6	-231.6	-184.7 (41%)	1.91	1.93	2.08	2.16	2.37 (25%)

*The final increase (in %) in the reported value at applied SMF of 100 AFU is given in parentheses.

Table 2. Distribution of the charge density [a.u.] at particular atoms of the methanol molecule depending on the applied SMF flux density [AFU].

Atom	Charge density [a.u.] at SMF flux density [AFU]					
	Tendency ^b	0	0.1	1.0	10	100
C1	V	-0.127	-0.105	-0.162	-0.137	-0.077
O2	RH	-0.739	-0.737	-0.688	-0.671	-0.610
H(3–5)	V	0.156	0.146	0.161	0.151	0.120
H6	V	0.398	0.404	0.367	0.355	0.326

^aData taken for drawing the average value for two or more either atoms or bonds are given in bold. ^bAbbreviations: RH – regularly increasing, RL – regularly decreasing, IH – irregularly increasing, IL – irregularly decreasing, V – lack of any regular tendency.

Table 3. Bond lengths [Å] in the methanol molecule depending on the applied SMF flux density [AFU].

Bond	Bond length [Å] at applied SMF flux density [AFU]					
	Tendency	0	0.1	1.0	10	100
C1-O2	IL	1.430	1.393	1.365	1.353	1.354
C1-H(3–5)	RH	1.090	1.167	1.178	1.213	1.328
O2-H6	IH	0.960	1.055	1.033	1.073	1.137

^aSee Table 2 for notation.

Table 4. Distribution of the charge density [a.u.] at particular atoms of the ethanol molecule depending on the applied SMF flux density [AFU].

Atom	Charge density [a.u.] at SMF flux density [AFU]					
	Tendency	0	0.1	1.0	10	100
C1	H	-0.079	-0.062	-0.024	0.053	0.196
C2	V	-0.662	-0.570	-0.548	-0.587	-0.550
O3	L	-0.684	-0.692	-0.702	-0.725	-0.753
H(4-5)	L	0.181	0.176	0.158	0.120	0.051
H(6-8)	IL	0.210	0.197	0.190	0.187	0.190
H9	H	0.374	0.381	0.390	0.407	0.434

*See Table 2 for notation.

Table 5. Bond lengths [\AA] in the molecule of ethanol depending on the applied SMF flux density [AFU].

Bond	Bond length [\AA] at applied SMF flux density [AFU]					
	Tendency	0	0.1	1.0	10	100
C1-C2	IL	1.540	1.520	1.500	1.495	1.528
C1-O3	L	1.430	1.418	1.394	1.389	1.252
C1-H(4-5)	H	1.090	1.098	1.142	1.222	1.352
C2-H(6-8)	IH	1.090	1.143	1.171	1.178	1.155
O3-H9	H	0.960	0.963	0.986	1.021	1.130

*See Table 2 for notation.

Table 6. Distribution of the charge density [a.u.] at particular atoms of the propan-1-ol molecule depending on the applied SMF flux density [AFU].

Atom	Charge density [a.u.] at SMF flux density [AFU]					
	Tendency	0	0.1	1.0	10	100
C1	IH	-0.047	-0.091	-0.015	0.155	0.129
C2	IL	-0.449	-0.441	-0.441	-0.411	-0.467
C3	IH	-0.594	-0.573	-0.567	-0.597	-0.483
O4	L	-0.687	-0.696	-0.705	-0.733	-0.785
H(5-6)	IL	0.178	0.176	0.172	0.088	0.169
H(7-8)	IL	0.223	0.215	0.213	0.193	0.201
H(9-11)	L	0.201	0.192	0.191	0.183	0.159
H12	H	0.373	0.378	0.386	0.415	0.438

*See Table 2 for notation.

Table 7. Bond lengths [\AA] in the molecule of propan-1-ol depending on the applied SMF flux density [AFU].

Bond	Bond length [\AA] at applied SMF flux density [AFU]					
	Tendency	0	0.1	1.0	10	100
C1-C2	IL	1.540	1.521	1.508	1.517	1.526
C2-C3	L	1.540	1.529	1.518	1.445	1.375
C3-O4	L	1.430	1.418	1.407	1.318	1.290
C1-H(5-6)	H	1.075	1.088	1.093	1.299	1.161
C2-H(7-8)	IH	1.090	1.125	1.128	1.252	1.186
C3-H(9-11)	H	1.090	1.127	1.140	1.216	1.286
O4-H12	H	0.960	0.962	0.968	1.061	1.102

*See Table 2 for notation.

In propan-2-ol (Tables 8, 9), in butan-1-ol (Tables 10, 11), in *S*-butan-2-ol (Tables 12, 13), in *iso*-butanol (Tables 14, 15) and in *tert*-butanol (Table 16, 17)

The visualisation of the shapes of those molecules at varying SMF flux density are presented in Figs 2–9.

Table 8. Distribution of the charge density [a.u.] at particular atoms of the propan-2-ol molecule depending on the applied SMF flux density [AFU].

Atom	Charge density [a.u.] at SMF flux density [AFU]					
	Tendency	0	0.1	1.0	10	100
C1	H	0.064	0.077	0.093	0.097	0.136
C(2–3)	IH	-0.584	-0.542	-0.526	-0.537	-0.508
O4	IH	-0.683	-0.686	-0.675	-0.672	-0.523
H5	V	0.191	0.177	0.170	0.182	0.174
H(6–8)	L	0.208	0.190	0.190	0.175	0.171
H(9–11)	V	0.199	0.188	0.178	0.201	0.191
H(6–8)&H(9–11)	IL	0.203	0.189	0.184	0.188	0.181
H12	IL	0.373	0.381	0.365	0.358	0.192

^aSee Table 2 for notation.

Table 9. Bond lengths [\AA] in the molecule of propan-2-ol depending on the applied SMF flux density [AFU].

Bond	Bond length [\AA] at applied SMF flux density [AFU]					
	Tendency	0	0.1	1.0	10	100
C1-C(2–3)	V	1.540	1.577	1.514	1.518	1.391
C1-O4	L	1.430	1.414	1.379	1.353	1.325
C1-H5	IH	1.090	1.142	1.164	1.152	1.189
C2-H(6–8)	H	1.090	1.172	1.186	1.194	1.280
C3-H(9–11)	IH	1.090	1.139	1.171	1.188	1.142
C2-H(6–8)&C3-H(9–11)	H	1.090	1.155	1.179	1.191	1.211
O4-H12	IH	0.960	0.925	1.045	1.084	1.610

^aSee Table 2 for notation.

Table 10. Distribution of the charge density [a.u.] at particular atoms of the butan-1-ol molecule depending on the applied SMF flux density [AFU].

Atom	Charge density [a.u.] at SMF flux density [AFU]					
	Tendency	0	0.1	1.0	10	100
C1	H	-0.050	-0.007	0.077	0.143	0.200
C2	V	-0.425	-0.399	-0.404	-0.390	-0.405
C3	V	-0.408	-0.396	-0.416	-0.393	-0.317
C4	V	-0.574	-0.500	-0.532	-0.506	-0.521
O5	L	-0.688	-0.699	-0.728	-0.766	-0.705
H(6–7)	L	0.178	0.161	0.125	0.109	0.103
H(8–9)		0.221	0.205	0.204	0.191	0.175
H(10–11)	IL	0.204	0.183	0.191	0.172	0.124
H(12–14)	V	0.199	0.173	0.187	0.180	0.187
H15	IL	0.372	0.382	0.404	0.427	0.386

^aSee Table 2 for notation.

Table 11. Bond lengths [\AA] in the molecule of butan-1-ol depending on the applied SMF flux density [AFU].

Bond	Bond length [\AA] at applied SMF flux density [AFU]					
	Tendency	0	0.1	1.0	10	100
C1-C2	V	1.540	1.516	1.512	1.536	1.576
C2-C3	L	1.540	1.529	1.504	1.448	1.378
C3-C4	IL	1.540	1.510	1.489	1.486	1.491
C1-O5	L	1.430	1.405	1.344	1.291	1.256
C1-H(6-7)	H	1.090	1.129	1.206	1.234	1.267
C2-H(8-9)	H	1.090	1.155	1.158	1.219	1.297
C3-H(10-11)	IH	1.090	1.178	1.168	1.205	1.372
C4-H(12-14)	V	1.090	1.215	1.155	1.177	1.153
O5-H15	H	0.950	0.983	1.022	1.089	1.486

*See Table 2 for notation.

Table 12. Distribution of the charge density [a.u.] at particular atoms of the *S*-butan-2-ol molecule depending on the applied SMF flux density [AFU].

Atom	Charge density [a.u.] at SMF flux density [AFU]					
	Tendency ^a	0	0.1	1.0	10	100
C1	V	-0.575	-0.503	-0.513	-0.517	-0.553
C2	IL	0.086	0.087	0.067	0.009	-0.176
C3	V	-0.435	-0.397	-0.428	-0.477	-0.313
C4	V	-0.601	-0.525	-0.545	-0.521	-0.538
O5	RH	-0.689	-0.673	-0.665	-0.627	-0.589
H(6-8)	V	0.207	0.183	0.188	0.186	0.217
H9	V	0.189	0.174	0.188	0.245	0.288
H10	V	0.203	0.183	0.202	0.198	-0.045
H11	V	0.223	0.202	0.212	0.211	0.285
H(12-14)	V	0.198	0.190	0.179	0.189	0.207
H15	IL	0.383	0.383	0.379	0.355	0.366

*See Table 2 for notation.

Table 13. Bond lengths [\AA] in the molecule of *S*-butan-2-ol depending on the applied SMF flux density [AFU].

Bond	Bond length [\AA] at applied SMF flux density [AFU]					
	Tendency ^a	0	0.1	1.0	10	100
C1-C2	IL	1.540	1.521	1.505	1.466	1.494
C2-C3	V	1.540	1.555	1.583	1.569	1.382
C3-C4	V	1.540	1.501	1.478	1.502	1.459
C1-H(6-8)	IH	1.090	1.200	1.171	1.186	1.307
C2-O5	RH	1.430	1.435	1.443	1.522	2.105
C2-H9	V	1.090	1.151	1.134	1.188	1.150
C3-H10	V	1.090	1.188	1.141	1.211	1.861
C3-H11	V	1.090	1.185	1.145	1.193	1.177
C3-H(12-14)	IL	1.090	1.200	1.190	1.177	1.157
O5-H15	IH	0.960	0.968	0.990	1.081	0.933

*See Table 2 for notation.

Table 14. Distribution of the charge density [a.u.] at particular atoms of the *iso*-butanol molecule depending on the applied SMF flux density [AFU].

Atom	Charge density [a.u.] at SMF flux density [AFU]					
	Tendency	0	0.1	1.0	10	100
C1	IH	-0.020	0.064	0.083	0.127	0.069
C2	V	-0.345	-0.391	-0.385	-0.374	-0.515
C(3–4)	IH	-0.550	-0.504	-0.513	-0.418	-0.251
O5	RL	-0.688	-0.700	-0.719	-0.738	-0.756
H(6–7)	V	0.178	0.132	0.133	0.140	0.203
H8	V	0.230	0.220	0.221	0.211	0.305
H(9–11)	RL	0.202	0.197	0.190	0.172	0.089
H(12–14)	RL	0.198	0.181	0.181	0.147	0.099
H(9–11)&H(12–14)	RL	0.200	0.189	0.185	0.159	0.094
H15	RH	0.375	0.392	0.397	0.405	0.428

^aSee Table 2 for notation.

Table 15. Bond lengths [\AA] in the molecule of *iso*-butanol depending on the applied SMF flux density [AFU].

Bond	Bond length [\AA] at applied SMF flux density [AFU]					
	Tendency	0	0.1	1.0	10	100
C1-C2	V	1.540	1.518	1.512	1.538	1.551
C2-C3	V	1.540	1.536	1.534	1.494	1.440
C3-C4	V	1.540	1.532	1.515	1.471	1.500
C1-O5	RL	1.430	1.406	1.366	1.294	1.081
C1-H(6–7)	IL	1.090	1.215	1.193	1.186	1.103
C2-H8	V	1.090	1.155	1.148	1.228	1.171
C3-H(9–11)	IH	1.090	1.176	1.163	1.227	1.857
C4-H(12–14)	IH	1.090	1.172	1.170	1.332	2.051
C3-H(9–11)&C4-H(12–14)	IH	1.090	1.174	1.167	1.279	1.954
O5-H15	V	0.960	0.955	1.018	1.131	1.104

^aSee Table 2 for notation.

Table 16. Distribution of the charge density [a.u.] at particular atoms of the *tert*-butanol molecule depending on the applied SMF flux density [AFU].

Atom	Charge density [a.u.] at SMF flux density [AFU]					
	Tendency	0	0.1	1.0	10	100
C1	V	0.162	0.169	0.172	0.177	0.092
C(2–4)	IH	-0.551	-0.502	-0.516	-0.474	-0.373
O5	V	-0.684	-0.683	-0.694	-0.696	-0.689
H(6–14)	IL	0.200	0.183	0.189	0.174	0.100
H15	H	0.371	0.370	0.375	0.376	0.387

^aSee Table 2 for notation.

Discussion

SMF turned negative values of heat of formation of alcohols less negative. It meant that SMF destabilised these molecules. That effect was accompanied with an increase in dipole moment (Table 1). The length of the carbon chain appeared to be crucial for the magnitude of those effects. Performed numerical simulations revealed that alcohols dis-

Table 17. Bond lengths [\AA] in the molecule of *tert*-butanol depending on the applied SMF flux density [AFU].

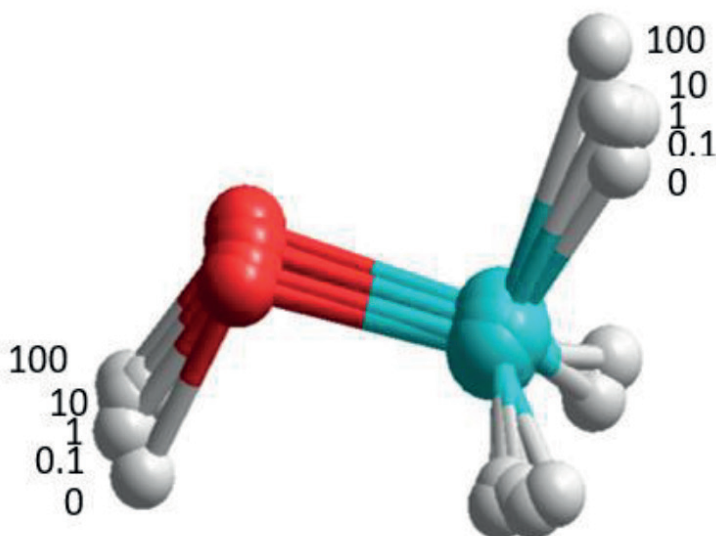
Bond	Tendency	Bond length [\AA] at applied SMF flux density [AFU]				
		0	0.1	1.0	10	100
C-C	RL	1.540	1.533	1.530	1.524	1.504
C-H	IH	1.090	1.166	1.163	1.229	1.542
C1-O5	IL	1.430	1.421	1.411	1.386	1.397
O5-H15	IH	0.960	0.984	0.969	1.006	1.013

^aSee Table 2 for notation.

Methanol Ethanol Propan-1-ol

Propan-2-ol Butan-1-ol *S*-(+)-Butan-2-ol

iso-Butanol *tert*-Butanol

**Figure 2.** Visualisation of the conformational changes of the methanol molecule structure produced by SMF of increasing flux density.

tinguished from one another in their expressed heat of formation and dipole moment sensitivity to increased SMF flux density. It is shown by corresponding orders of those parameters arranged, based on the effect observed at SMF flux density at 100 AFU.

Order of sensitivity of heat of formation:

Methanol > Butan-1-ol > *tert*-Butanol > Ethanol > *iso*-Butanol > Propan-1-ol > *S*-Butan-2-ol > Propan-2-ol

Order of sensitivity of dipole moment:

Methanol > Ethanol > *S*-Butan-2-ol > Propan-1-ol > Butan-1-ol > *tert*-Butanol > *iso*-Butanol > Propan-2-ol

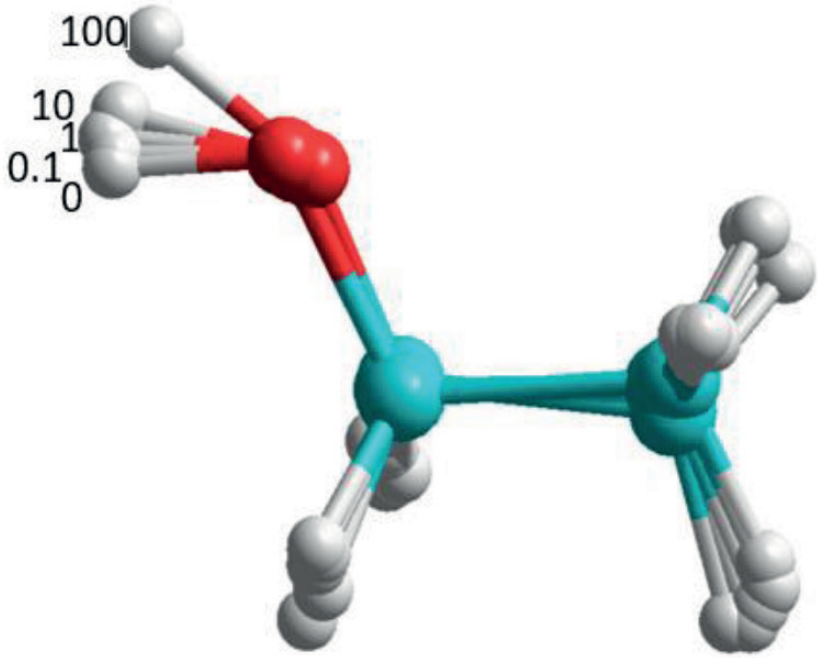


Figure 3. Visualisation of the conformational changes of the ethanol molecule structure produced by SMF of increasing flux density.

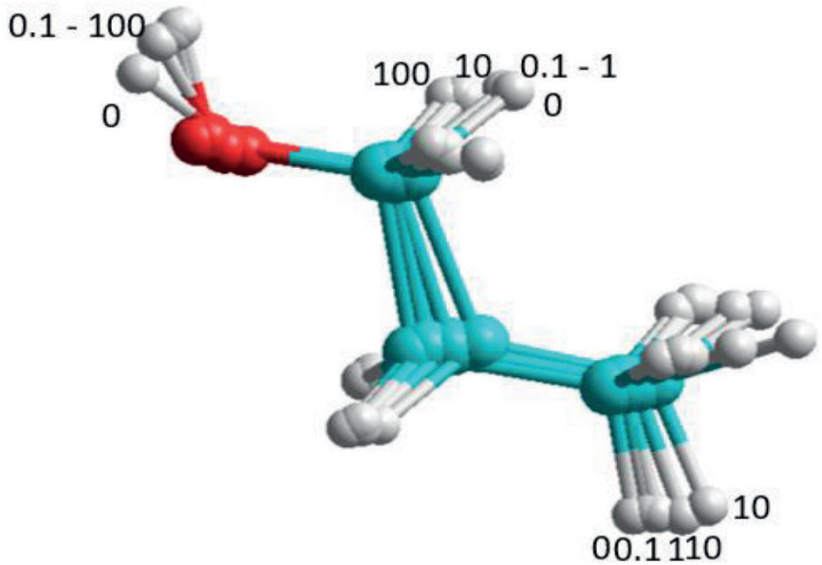


Figure 4. Visualisation of the conformational changes of the propan-1-ol molecule structure produced by SMF of increasing flux density.

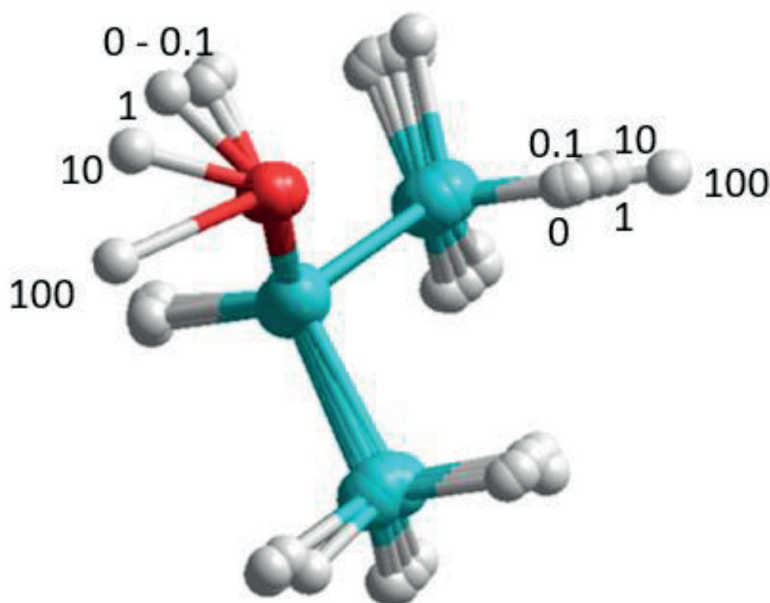


Figure 5. Visualisation of the conformational changes of the propan-2-ol molecule structure produced by SMF of increasing flux density.

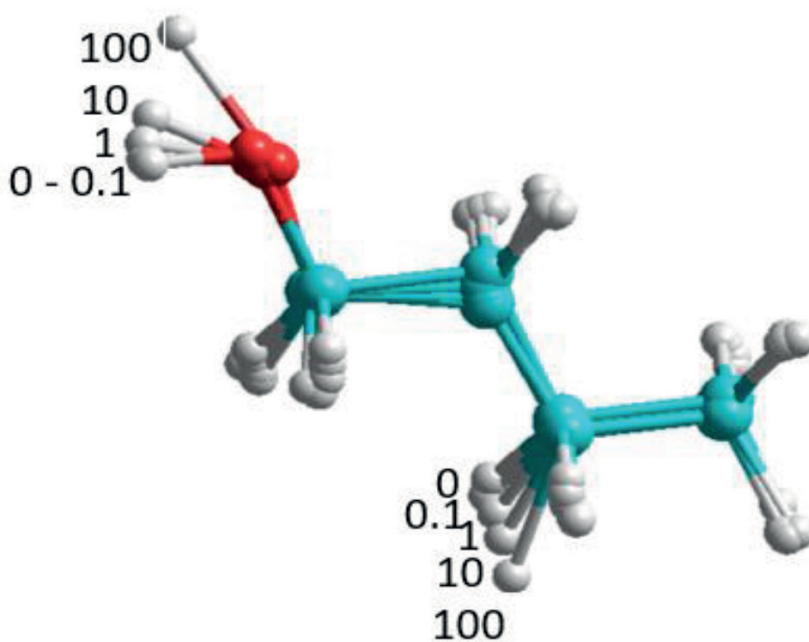


Figure 6. Visualisation of the conformational changes of the butan-1-ol molecule structure produced by SMF of increasing flux density.

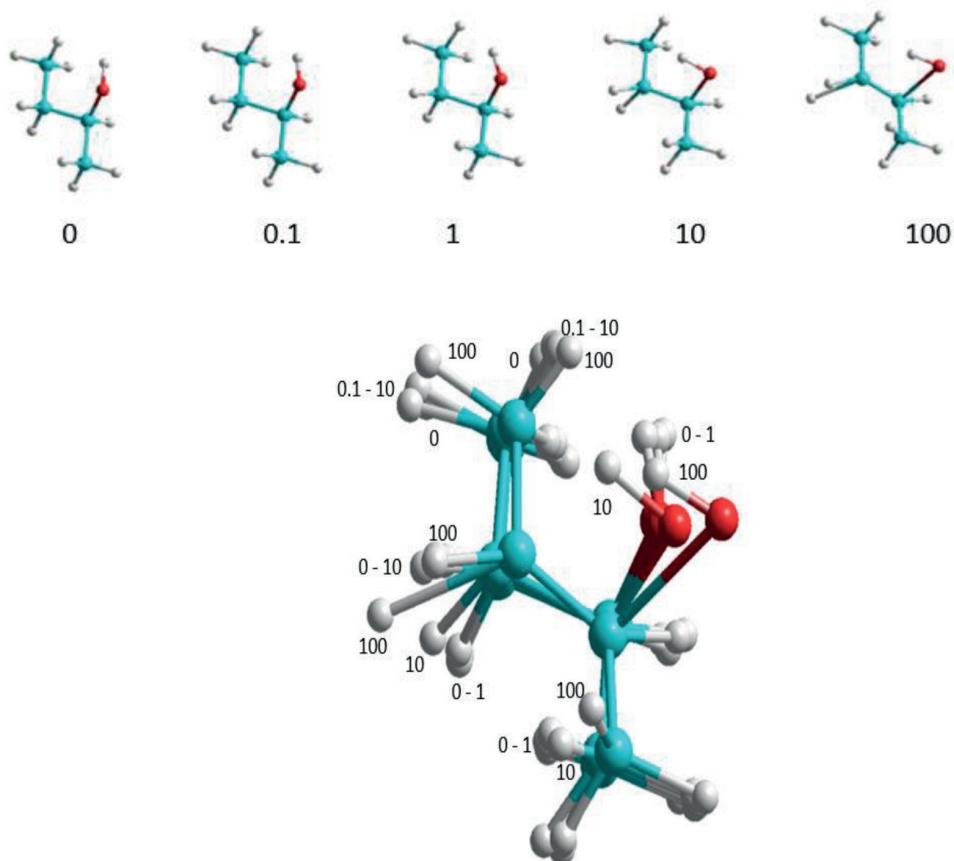


Figure 7. Visualisation of the conformational changes of the structure of *S*-butan-2-ol molecule produced by SMF of increasing flux density.

For instance, at 100 AFU, the heat of formation and dipole moment rose by approximately 49% and 55%, respectively. Under the same accepted conditions, these parameters for butan-1-ol rose by approximately 42% and 26%, respectively. Results of the simulations showed that the sensitivity of the alcohols to the applied SMF changed irregularly against the length of the carbon chain (Table 1). Such behaviour pointed to an involvement of complex factors. It is likely that they included changes in the conformation of the carbon chains, bond lengths and bond angles leading to repulsion of some fragments of the structure of those molecules away from the direction of the applied SMF. Such behaviour could evoke variable electrostatic and polar interactions through space, between particular atoms of the molecules.

These postulates were then recognised separately for particular alcohols under consideration (Fig. 1).

In the methanol molecule, because of the polarisation of the C-H bonds, the C1 atom took the negative charge. Its density changed irregularly with an increase in the

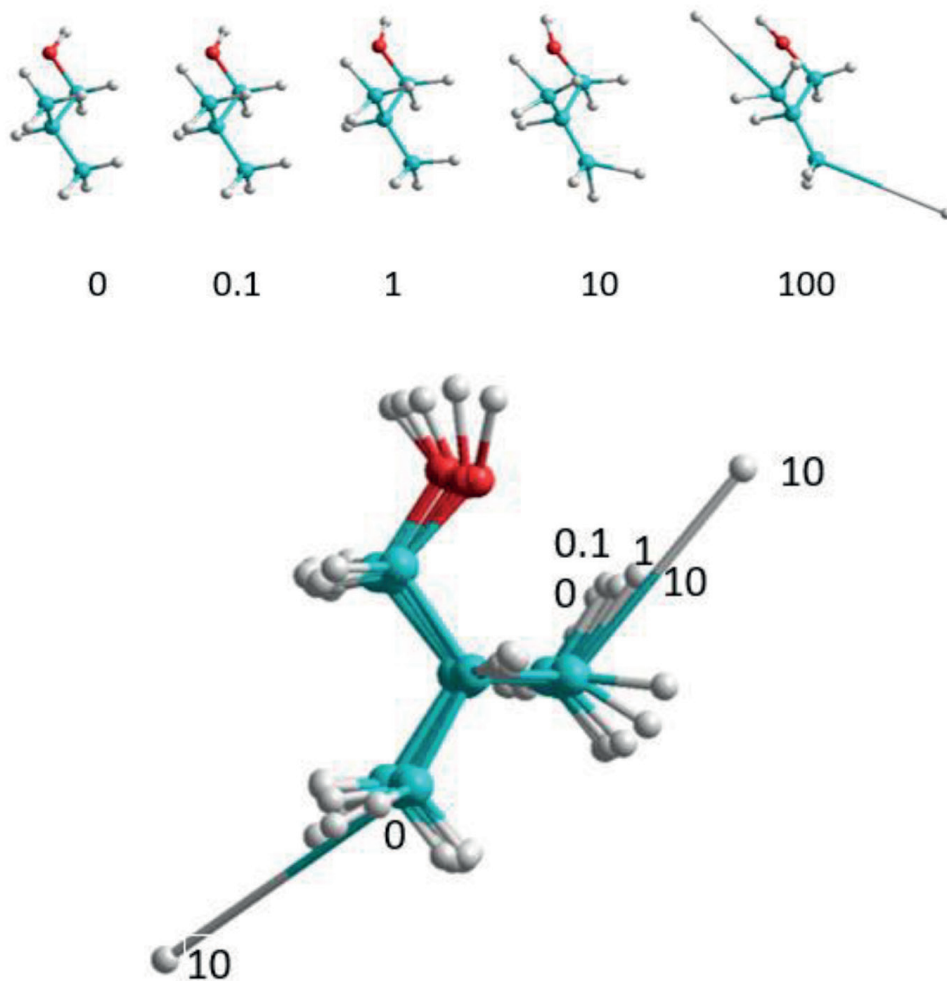


Figure 8. Visualisation of the conformational changes of the structure of *iso*-butanol molecule produced by SMF of increasing flux density.

SMF flux density. Initially, at 0.1 AFU, it decreased possibly due to polarisation of the C-O bond caused by the electron accepting properties of the O2 atom. The highest negative charge density at the C1 atom was noted at 1.0 AFU and substantially declined regularly up to 100 AFU (Table 2). Since the negative charge density at the O2 atom fairly regularly declined with an increase in AFU, the observed regularity should result from the C1-H interactions. Due to free rotation around the C1-O2 bond all three hydrogen atoms (H3, H4 and H5) of the methyl group are, in fact, equivalent to one another. However, the rules accepted in situating that molecule in the magnetic field cancelled that equivalence. Therefore, in Table 2, computed values of the charge density of those atoms were not identical. In order to omit that in consequence, the average of those three parameters was discussed. The average positive charge density

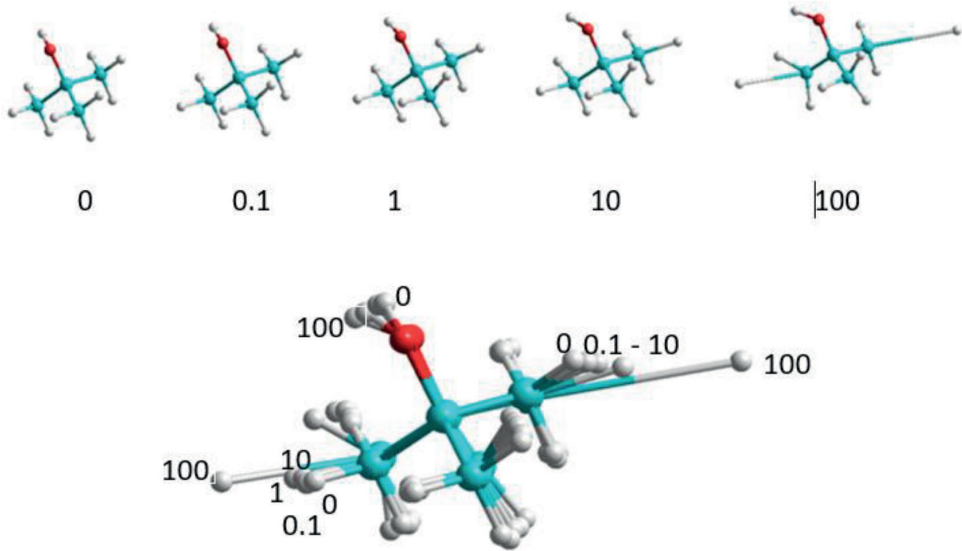


Figure 9. Visualisation of the conformational changes of the structure of the *tert*-butanol molecule produced by SMF of increasing flux density.

at the H3-H5 atoms and at the H6 atom irregularly decreased with an increase in the SMF flux density. These changes could originate from pushing particular hydrogen atoms out of the magnetic field. In Table 3, the bond lengths between particular atoms revealed a general tendency of the shortening the C1-O2 bond with an increase in applied SMF. This behaviour was observed in spite of simultaneous declining of the negative charge at those atoms. The length of the remaining bonds increased although slight irregularities in the case of the C1-(H3-H5) and O2-H6 bonds, in both cases taking place at 1 AFU were noted. The visualisation of the shapes of the molecule at varying SMF flux density (Fig. 2) confirmed that the irregularities could result from slight mobility of the molecule placed in the magnetic field and subtle changes of the bond angles.

In the ethanol molecule without SMF, both the C1 and C2 atoms were negatively charged (Table 4). As the applied SMF flux density increased, the charge density at both atoms declined. That at the C1 atom reached positive charge already at 10 AFU. It could rationalise the increase in the negative charge density at the O3 atom. Under SMF, the latter atom polarised not only the C1-O3, but also the O3-H9 bond. In consequence, the positive charge density at the H9 atom rose with an increase in the flux density. As the result of the decrease in the electronegativity of the C1 atom, the positive charge density at the H4 and H5 atoms declined. Declining with increasing flux density electronegativity of the C2 atom resulted in a gradual decrease of the positive charge density at the H6, H7 and H8 atoms. The latter irregularity was reflected by irregular changes in the C2-H6 bond (Table 5). Under the influence of SMF, the length of the C1-C2 and C1-O3 bonds declined with an increase in the applied flux

density. Simultaneously, the length of all C-H bonds and the O3-H9 bond increased with the flux density applied.

The visualisation of the ethanol molecule placed in SMF with increased flux density (Fig. 3) demonstrated the slight conformational changes in the initial position of the molecule out of the field. The essential change of the position of the H9 atom corresponded to observed irregularity in the C1-C2 bond length at 100 AFU.

In the charge density distribution in the propan-1-ol molecule SMF of increasing flux density generated many more irregularities. They were caused mainly by SMF of 100 AFU although some irregularities were noted also in the charge density at the C1 atom at 0.1 AFU, at the C3 atom at 10 AFU and the H(5-6) atom at 10 AFU (Table 6). All three carbon atoms in this alcohol were negatively charged. In the SMF of increasing flux density, the negative charge density at all carbon atoms declined. The C2 and C3 carbon atoms retained that charge also at 100 AFU, but the C1 atom turned into positively charged already at 10 AFU. Since with an increase in the flux density, the O4 atom turned more electron attracting, this phenomenon could be rationalised in a similar manner as presented for ethanol. The positive charge density at the H12 atom regularly rose, likely as the consequence of increasing electronegativity of the O4 atom. In contrast to that, the positive charge density declined with an increase in the flux density at the H(5-6), H(7-8) and H(9-11) atoms at the flux density up to 100 AFU. In the two first cases, it declined solely up to 10 AFU and at 100 AFU it rose. In the case of the H(9-11) atoms, a possibility of their polar interaction with the O4 atom could eventually be taken into account, but visualisation of the shape of that molecule in the SMF (Fig. 4) did not support that assumption. The length of all C-C bonds, although irregularly in the case of the C1-C2 bond, decreased with an increase in the applied flux density (Table 7). The C3-O4 bond also shortened. All the C1-H(5-6) and C2-H(7-8) bonds regularly expanded up to 10 AFU in order to compress at 100 AFU. The C3-H(9-11) and the O4-H12 were regularly elongated up to 100 AFU.

The visualisation presented in Fig. 4 confirmed that observed effects originated from small movements of the molecule at increasing SMF intensity and associated changes in bond angles.

The carbon chain in the molecule of propan-2-ol was more capable of various conformational transformations involving the methyl groups. On the other hand, intervention of the intramolecular polar interactions was unlikely. It resulted in irregular responses of the charge density (Table 8) and bond lengths (Table 9) to the application of SMF and its increasing flux density. The C1 carbon atom holding the hydroxyl and two methyl groups was positively charged and the charge density regularly increased with an increase in the flux density. The C2 and C3 carbon atoms of both side methyl groups were negatively charged and these charges, even without SMF, were not identical. As the flux density rose, the charge density at both these atoms declined although it proceeded irregularly. This trend was accompanied by a fairly regular decrease of the negative charge density at the O4 atom. The positive charge density at the H5 - H11 atoms generally, although irregularly, decreased with increasing flux density. These rather subtle irregularities were observed at 10 AFU. The charge density at the

H12 atom declined regularly against the increasing flux density. The C1-C(2–3) bond length at 0.1 AFU increased in order to decrease up 100 AFU and, at the same time, the length of the C1-O4 bond decreased regularly. All the C-H bonds [C2-H(6–8) & C3-H(9–11) av.] and O-4-H12 bonds increased their lengths with increasing flux density although the latter bond did it irregularly at 0.1 AFU. Fig. 5 demonstrates the origin of those irregularities. They were changes in bond angles and subtle re-orientations in the original position along the x-axis.

As in case of results of computations for ethanol and propan-1-ol, such computations for normal carbon chain butan-1-ol delivered the scope of data with very few irregularities in the flux density dependent on changes of charge density (Table 10) and bond lengths (Table 11).

Out of SMF, the C1-carbon atom holding the hydroxyl group was weakly negatively charged. As the flux density of the applied SMF increased, the charge of that atom turned to positive and its value increased regularly with increasing flux density. All remaining carbon atoms of the chain were negatively charged and their charge density fairly regularly decreased with an increase in the flux density applied. Amongst them, the C3 atom was the least electronegative and, at 1.0 AFU, its electronegativity jumped considerably. The electronegativity of the O5 atom increased with an increase in the flux density up to 10 AFU and regularly decreased up to 100 AFU. The positive charge density at the H6 – H10 and H14 atoms fairly regularly decreased with an increase in the flux density, whereas the charge density at the H11-H13 atoms irregularly increased. The positive charge density at the H15 atom belonging to the hydroxyl group regularly increased up to 10 AFU and declined regularly up to 100 AFU. The length of the C1-C2 bond, initially at 0.1, 1 and 10 AFU, decreased and then increased regularly up to 100 AFU. The length of C2-C3, C3-C4 and C1-O5 bonds at that time declined. The bond length of all C-H bonds and the O5-H14 group increased with an increase in flux density. That increase became irregular in the case of the terminal methyl group (Table 11). The visualisation of the structural changes in the butan-1-ol molecule evoked by applied SMF (Fig. 6) points to the same factors rationalising the results of computations. Additionally, the polar interactions between the hydrogen atoms of the H10 atom, particularly at 100 AFU, seems to be likely.

Butan-2-ol called also *sec*-butanol exists in two, *R* and *S* enantiomers. The *S* enantiomer is more common. The asymmetry centre at the C2 atom did not influence the results of computations, thus, data collected in Tables 12, 13 were valid for both enantiomers. Due to the asymmetry centre located at the C2 atom, the H10 and H11 atoms and the C3-H10 and C3-H11 were not equivalent to one another, respectively. Therefore, corresponding values were not average. Except for the C2 carbon atom, the remaining carbon atoms in that molecule carried a negative charge density although, at 100 AFU, the C2 atom also took the negative charge density. Increasing flux density decreased that negative charge. Additionally, the negative charge density at the O5 atom behaved similarly. Except for the H10 atom which carried the negative charge density at 100 AFU, all remaining carbon atoms carried the positive charge density. Its value varied highly irregularly with increasing flux density (Table 12). These facts pointed to a considerable role of conformational changes within that molecule and

intramolecular polar interactions. Solely the C2-O5 bond length regularly increased with the flux density. The lengths of the other bonds varied irregularly (Table 13).

The visualisation of the structural changes in the *S*-butan-2-ol molecule evoked by applied SMF (Fig. 7) pointed to the same factors rationalising the results of computations. Additionally, the polar interactions between the hydrogen atoms of the H10 atom, particularly at 100 AFU, seemed to be likely.

For the same reasons as mentioned in case of propanol-2-ol, computed changes in the charge density (Table 14) and bond length in the *iso*-butanol fairly irregularly changed with an increase in the SMF flux density. The residual electronegativity of the C1 atom in the molecule out of SMF ceased already at 0.1 AFU. The positive charge at that atom rose up to 10 AFU and slightly declined regularly up to 100 AFU. The electronegativity of the C2 increased with the flux density in contrast to that of the C3 and C4 atoms whose electronegativity was reduced. Simultaneously, the electronegativity of the O5 atom regularly increased. The flux density of 100 AFU considerably increased the positive charge density at the H8 and H15 atoms. The positive charge density at the remaining H- atoms, except for the H6 and H7 atoms, declined under the influence of lower flux densities (Table 14). There were also numerous irregularities in the influence of increasing flux density upon the bond lengths. The length of the C1-C2 bond initially decreased in order to increase again at 10 AFU and the C2-C3, C3-C4 and C1-O5 bonds were shortened. Simultaneously, all the C-H bonds expanded, some of them irregularly against increasing flux density (Table 15). The visualisation of the effects of SMF upon the structure of the *iso*-butanol molecule (Fig. 8) suggested possible intervention in the structure modification from intramolecular polar interactions involving the H10 hydrogen and O5 atoms.

The highly-branched carbon chain of *tert*-butanol provided three methyl groups. Potentially, they could change their orientation in SMF, controlled by the generated variable positive charge density located at a particular hydrogen atom at a given flux density. That factor could rationalise irregular changes of charge densities at particular atoms (Table 16) and bond lengths (Table 17) on increasing flux density. Thus, for instance, the positive charge density at the C1 atom rose up regularly to decline at 100 AFU. The negative charge density at the equivalent C2, C3 and C4 atoms also declined with an increase in the flux density. Increasing flux density only slightly influenced the negative charge density at the O5 oxygen atom. The positive charge density of the carbon bound hydrogen atoms fairly regularly declined against increasing flux density, whereas the positive charge density located at the O5 atom bound to the hydrogen atom slightly, but regularly increased. These effects contributed to irregular changes of the bond lengths presented in Table 17. The observed irregularities could also result from perturbations in rotation of the vicinal groups caused by electrostatic repulsion of the hydrogen atoms through space. The length of the C-C- and C1-O5 bonds decreased with an increase in the flux density, whereas, simultaneously, the length of the C-H and O5-H15 bonds increased (Table 17). Fig. 9 presents conformational changes evoked by SMF in the molecule of *tert*-butanol.

A rigid molecule situated in respect to the direction of the magnetic field resulted in diamagnetic interactions with electrons of the bonds. Thus, these interactions could

be reflected by elongation of the bonds instead of moving in the space. This is known as a phenomenon of levitating living frogs observed in SMF on the level of 12–20T (Berry 1997) (≈ 0.012 – 0.02 AFU) and these remaining healthy after experiments.

In performed computations, a decrease in heat of formation of alkanols with an increase in applied SMF flux density accompanied with increase in dipole moments pointed to weakening the bonds and, at the same time, elongation of the bonds. It resulted from the destabilising effect of SMF upon spin-paired electrons. Inspection of the alkanols geometry changing with SMF arranged parallel to the long axis of the molecules showed that, in several cases, the effect of the bond elongation is the strongest when the bond and direction of the field force lines reached approximately the 45° angle. It was noted for the molecules of methanol, butan-1-ol, *S*-butan-2-ol, *iso*-butanol and *tert*-butanol.

Biological function of alcohols in organisms of flora and fauna chiefly involves the hydroxyl group. That group is attacked by various enzymes metabolising alcohols via a complex catabolic and metabolic pathway (US Department of Health & Human Services 2007; Vaswami 2019). In the first step, the hydroxyl group of alcohol plays a role of the Lewis base. Hence the high negative charge density at the oxygen atom of that group favours the initial step of the alcohol metabolism. Simultaneously, elongation of the O-H bond should favour the contact of the alcohol with attacking enzymes. Taking these arguments into account, based on the insight in particular Tables, one could state that SMF declined the Lewis basicity, that is, inhibited reaction with enzymes in methanol, propan-2-ol and *S*-butan-2-ol. Except for methanol, the alkanols bearing their hydroxyl groups at the terminal CH_2 group of the chain were stimulated by SMF to react with enzymes. Amongst the SMF stimulated alkanols, the *tert*-butanol was least sensitive. The length of the O-H bond increased in all cases.

Taking into account the chemical oxidation of alkanols, attention should be paid to the response of the positive charge density at the hydrogen atom bound to the carbon atom holding also the hydroxyl group to an increase in the applied SMF flux. One could see that, in the molecules of methanol, ethanol, propan-1-ol, propan-2-ol and butan-1-ol, the positive charge density decreased making that hydrogen atom less acidic. Only in *S*-butan-2-ol and isobutanol, this charge density varied very chimerically. *tert*-Butanol did not possess such a hydrogen atom. A decrease in the positive charge at the geminal hydrogen atom made it more sensitive to the reactions of the free radical mechanism that is less susceptible to the reactions involving the ionic mechanism.

Conclusions

Static magnetic field of flux density increasing from 0 to 100 AFU destabilised the molecules of alkanol as shown by the increasing heat of formation of those molecules and their dipole moment.

SMF produced an increase in the negative charge density at the oxygen atom of the hydroxyl group and elongated the $-\text{O}-\text{H}$ bond length. These results show that SMF facilitates metabolism of the alkanols.

Some irregularities in the changes of positive and negative charge densities and bond lengths provide evidence that molecules slightly change their initially fixed positions in respect to the force lines of the magnetic field. Length of some bonds and bond angles change with an increase in the applied flux density providing, in some cases, polar interactions between atoms through the space.

SMF flux density initially defined in T evoked much stronger effects than could be anticipated, based on the comparative analysis with experimental results of flux density. Computations were performed for extremely high intensity of SMF at which almost every molecule and every element of construction could be destroyed. In natural Earth conditions, generated SMF of hardly 2 AFU destroyed electromagnetism within milliseconds. Thus, introduced AFU were at 1000 times higher than T. Hence, results of effects of SMF to humans predicted in this paper are purely theoretical in contrast to effects of alternating electromagnetic fields of much lower intensity.

References

- Andreini C, Bertini I, Cavallaro G, Holliday GL, Thornton JM (2008) Metal ions in biological catalysis: From enzyme databases to general principles. *Journal of Biological Inorganic Chemistry* 13(8): 1205–1218. <https://doi.org/10.1007/s00775-008-0404-5>
- Bao S, Guo W (2021) Transient heat transfer of superfluid ^4He in nonhomogeneous geometries: Second sound, rarefaction, and thermal layer. *Physical Review B* 103(13): e134510. <https://doi.org/10.1103/PhysRevB.103.134510>
- Beretta G, Mastorgio AF, Pedrali L, Saponaro S, Sezenna E (2019) The effects of electric, magnetic and electromagnetic fields on microorganisms in the perspective of bioremediation. *Reviews in Environmental Science and Biotechnology* 18(1): 29–75. <https://doi.org/10.1007/s11157-018-09491-9>
- Berry MV, Geim AK (1997) Of flying frogs and levitrons. *European Journal of Physics* 18(4): 307–313. <https://doi.org/10.1088/0143-0807/18/4/012>
- Buchachenko A (2009) *Magnetic isotope effect in chemistry and biochemistry*. Nova Science Publisher, NY.
- Buchachenko LA (2014) Magnetic control of enzymatic phosphorylation. *Journal of Physical Chemistry & Biophysics* 4: e1000142. <https://doi.org/10.4172/2161-0398.1000142>
- Buchachenko A (2016) Why magnetic and electromagnetic effects in biology are irreproducible and contradictory? *Bioelectromagnetics* 37(1): 1–13. <https://doi.org/10.1002/bem.21947>
- Buchachenko AL, Kuznetsov DA, Breslavskaya NN (2012) Chemistry of enzymatic ATP synthesis: An insight through the isotope window. *Chemical Reviews* 112(4): 2042–2058. <https://doi.org/10.1021/cr200142a>
- Carpenter JE, Weinhold F (1988) Analysis of the geometry of the hydroxymethyl radical by the different hybrids for different spins natural bond orbital procedure. *Journal of Molecular Structure (Theochem)* 139: 41–62. [https://doi.org/10.1016/0166-1280\(88\)80248-3](https://doi.org/10.1016/0166-1280(88)80248-3)
- Charistos ND, Muñoz-Castro A (2019) Double aromaticity of the B-40 fullerene: Induced magnetic field analysis of pi and sigma delocalization in the boron cavernous structure.

- Physical Chemistry Chemical Physics 21(36): 20232–20238. <https://doi.org/10.1039/C9CP04223G>
- Ciesielski W, Girek T, Oszczyda Z, Soroka JA, Tomasik P (2021) Towards recognizing mechanisms of effects evoked in living organisms by static magnetic field. Numerically simulated effects of the static magnetic field upon simple inorganic molecules. F1000 Research 10: e611. <https://doi.org/10.12688/f1000research.54436.1>
- Committee to Assess the Current Status and Future Direction of High Magnetic Field Science in the United States (2013) High Magnetic Field Science and Its Application in the United States; Current Status and Future Directions. Natl. Res. Council, National Acad., The National Academies Press, Washington, D.C.
- Dinan L, Harmatha J, Lafont R (2001) Chromatography procedures for isolation of plant steroids. Journal of Chromatography A 935(1–2): 105–122. [https://doi.org/10.1016/S0021-9673\(01\)00992-X](https://doi.org/10.1016/S0021-9673(01)00992-X)
- Farberovich OV, Mazalova VL (2016) Ultrafast quantum spin-state switching in the Co-octaethylporphyrin molecular magnet with a terahertz pulsed magnetic field. Journal of Magnetism and Magnetic Materials 405: 169–173. <https://doi.org/10.1016/j.jmmm.2015.12.038>
- Frisch MJ, Trucks GW, Schlegel HB, Frisch MJ, Trucks GW, Schlegel HB, Scuseria GE, Robb MA, Cheeseman JR, Scalmani G, Barone V, Mennucci B, Petersson GA (2016) Gaussian 09, Revision A.02, Gaussian, Inc., Wallingford.
- Froimowitz M (1993) HyperChem: A software package for computational chemistry and molecular modelling. BioTechniques 14: 1010–1013.
- Glendening ED, Reed AE, Carpenter JE (1987) Extension of Lewis structure concepts to open-shell and excited-state molecular species, NBO Version 3.1. Ph.D. thesis, University of Wisconsin, Madison, WI.
- Hamza A-SHA, Shaher SA, Mohmoud A, Ghania SM (2002) Environmental pollution by magnetic field associated with power transmission lines. Energy Conversion and Management 43(17): 2442–2452. [https://doi.org/10.1016/S0196-8904\(01\)00173-X](https://doi.org/10.1016/S0196-8904(01)00173-X)
- Jaworska M, Domański J, Tomasik P, Znój K (2014) Methods of stimulation of growth and pathogenicity of entomopathogenic fungi for biological plant protection. Polish Patent 223412.
- Jaworska M, Domański J, Tomasik P, Znój K (2016) Preliminary studies on stimulation of entomopathogenic fungi with magnetic field. Journal of Plant Diseases and Protection 12: 295–300. <https://doi.org/10.1007/s41348-016-0035-y>
- Jaworska M, Domański J, Tomasik P, Znój K (2017) Preliminary studies on stimulation of entomopathogenic nematodes with magnetic field. Prom. Zdr. Ekol 4(9).
- Kohno M, Yamazaki M, Kimura I, Wada M (2000) Effect of static magnetic fields on bacteria: *Streptococcus mutans*, *Staphylococcus aureus*, and *Escherichia coli*. Pathophysiology 7(2): 143–148. [https://doi.org/10.1016/S0928-4680\(00\)00042-0](https://doi.org/10.1016/S0928-4680(00)00042-0)
- Letuta UG, Berdinskiy VL (2017) Magnetosensitivity of bacteria *E. coli*: Magnetic isotope and magnetic field effects. Bioelectromagnetics 38(8): 581–591. <https://doi.org/10.1002/bem.22073>
- Lewis DH, Smith DC (1967) Sugar alcohols (polyols) in fungi and green plants. The New Phytologist 66(2): 143–184. <https://doi.org/10.1111/j.1469-8137.1967.tb05997.x>

- Marchand N, Lienard P, Siehl H, Izato H (2014) Applications of molecular simulation software SCIGRESS in industry and university. *Fujitsu Scientific and Technical Journal* 50(3): 46–51.
- Rankovic V, Radulovic J (2009) Environmental pollution by magnetic field around power lines. *International Journal of Qualitative Research* 3(3): 1–6.
- Rittie L, Perbal B (2008) Enzymes used in molecular biology: A useful guide. *Journal of Cell Communication and Signaling* 2(1–2): 25–45. <https://doi.org/10.1007/s12079-008-0026-2>
- Rowland O, Domerque F (2012) Plant fatty acyl reductases: Enzyme generating fatty alcohols for protective layers with potential for industrial applications. *Plant Science* 193–194: 28–38. <https://doi.org/10.1016/j.plantsci.2012.05.002>
- Steiner UE, Ulrich T (1989) Magnetic field effects in chemical kinetics and related phenomena. *Chemical Reviews* 89(1): 51–147. <https://doi.org/10.1021/cr00091a003>
- Tang Y, Guo W, Lvov W, Pomyalov A (2021) Eulerian and Lagrangian second-order statistics of superfluid ${}^4\text{He}$ grid turbulence. *Physical Review B* 103(14): e144506. <https://doi.org/10.1103/PhysRevB.103.144506>
- US Department of Health & Human Services (2007) Alcohol metabolism: An update. *Alcohol alert*: 72.
- Vaswami M (2019) ADH and ALDH polymorphism in alcoholism and alcohol misuse/dependence. In: Preedy VR (Ed.) *Neuroscience of Alcohol: Mechanism and Treatment*. Academic Press, London. <https://doi.org/10.1016/B978-0-12-813125-1.00004-0>
- Wade LG (2021) Alcohol chemical compounds. *Encyclopedia Britannica*. [Accessed 26 June 2021]
- Woodward JR (2002) Radical pairs in solution. *Progress in Reaction Kinetics and Mechanism* 27(3): 165–207. <https://doi.org/10.3184/007967402103165388>
- Woronowicz B (2003) *Without Secrets on Addictions and Their Therapy*. Ed. Instytut Psychiatrii i Neurologii, Warsaw. [in Polish]
- Zamiatała K, Domański J, Krystyjan M, Tomasiak P (2013) Effect of magnetic field upon selected cosmetics creams. *Polish Journal of Cosmetology* 16(2): 144–147.